

Table 1 Partial calculation results (change of pressure and coolant flow in re-entry process, time from 76.2 km, Tl coolant)

t	p_{in} , present	p_{in} , Ref. 2	Relative difference, %	\dot{M} , present	\dot{M} , Ref. 2	Relative difference, %
17.5	20.50	21.50	4.65	0.036	0.034	-5.88
18	40.00	45.00	11.11	0.054	0.049	-10.20
19	100.00	105.00	4.76	0.207	0.202	-2.48
20	195.00	200.00	2.50	0.464	0.463	-0.22
20.5	234.80	262.50	10.55	0.563	0.540	-4.26
22	212.48	212.50	0.01	0.473	0.459	-3.05
23	193.00	200.00	3.50	0.477	0.454	-5.07
24	187.00	190.00	1.57	0.346	0.360	-3.89
25	175.00	177.00	1.13	0.383	0.374	-2.41

Table 2 Partial calculation results of \dot{M} , Δp , and p_{in} for four coolants

Coolant	\dot{M}	Δp	p_{in}
Tl	4.5	92.90	192.90
In	2.01	62.44	162.44
Sn	1.92	70.55	170.55
H ₂ O	2.92	494.62	594.66

and for liquid coolant is

$$(p_{in})_{la} = \frac{q_{w0} \mu (\bar{R}_{ex} - \bar{R}_{in})}{\rho \Gamma L_v \left[1 + 0.6 (\bar{M}_a / \bar{M}_c)^{\frac{1}{3}} \right]} + p_{ex} \quad (24a)$$

$$(p_{in})_t = \frac{q_{w0} \mu (\bar{R}_{ex} - \bar{R}_{in})}{\rho \Gamma L_v \left[1 + 0.2 (\bar{M}_a / \bar{M}_c)^{\frac{1}{10}} \right]} + p_{ex} \quad (24b)$$

Calculation Examples

For a check of the validity of the simplified method, a computational example is given. According to the parameters of the re-entry orbit, the thermal protection of SCAT with four different physical character coolants is calculated.

The partial calculated results are given in Tables 1 and 2. It can be seen in Table 1 that, in the re-entry process, the present calculative results agree fairly well with the numerical computation of Ref. 2 for the pressure and coolant of thallium.

Table 2 shows the total coolant mass flow $\dot{M}_{Sn} < \dot{M}_{In} < \dot{M}_{H_2O} < \dot{M}_{Tl}$ and the internal pressure $p_{In} < p_{Sn} < p_{Tl} < p_{H_2O}$. The results of the computational example show that the thermal protection effect of coolant In is best and that the thermal protection effect of coolant H₂O is worst because the internal pressure (p_{H_2O}) is too high, destroying the porous nosetip. Thus, H₂O is an unacceptable coolant.

Conclusions

From the preceding results and analyses of calculation examples, we can derive the following conclusions.

1) The theoretical analysis method based on three simplified assumptions is dependable and accurate.

2) The simplified calculative results agree fairly well with the numerical computation of Ref. 2. The difference between the present simplified calculation and the numerical computation of Ref. 2 is about $\pm 0.01 \sim \pm 11\%$.

3) The present calculative method can be satisfactorily used for prediction before a ground simulation experiment, and it can be done at the request of an engineering application department.

References

- 1Fogaroli, R. P., and Laganelli, A. L., "The Effect of Mach Number and Wall Temperature on Turbulent Heat Blockage Resulting from Mass Injection," AIAA Paper 77-784, July 1977.
- 2Grinberg, I. M., Stellrecht, D. E., Whitacre, G. R., and Bagby, F. L., "Development of SCAT Nosetip Concept for Advanced Reentry Vehicles," U.S. Naval Surface Weapons Center, Silver Spring, MD, Jan. 1976.

T. C. Lin
Associate Editor

Performance of Diamond-Coated Silicon Nitride Bearings

M. D. Drory*

Crystallume, Santa Clara, California 95054

Introduction

SOLID lubrication of bearings for space applications, such as precision pointing mechanisms, has been proposed in recent years with the use of synthetic diamond coatings. Diamond is a reasonable candidate for a low-friction coating because it possesses exceptional corrosion resistance and a low coefficient of friction (except at ultra-high vacuum) with the highest values of hardness and stiffness.¹ In addition to the lubrication properties of diamond, the coating may improve the chemical/mechanical wear resistance of the base material. Coatings are applied to bearing elements for improving performance and prolonging life by enhancing the resistance to substrate spalling (galling) and lubricant degradation.²

Diamond may be a suitable low-friction and protective coating for bearings because it is available in thin film form by chemical vapor deposition (CVD) methods at low pressures ($130\text{--}1.3 \times 10^4$ Pa) and modest temperatures ($600\text{--}1000^\circ\text{C}$) (Ref. 3). An important aspect of the CVD process is the conformal coating of complex shapes, such as spheres. Much of the effort in our laboratory was directed toward obtaining surface characteristics of the diamond coating that are consistent with precision (silicon nitride) bearing components, such as the balls and rings.⁴ A conformal diamond has been obtained on 1–25-mm-diam silicon nitride balls.

A number of refractory materials can be diamond coated, such as most ceramics. However, as diamond growth is achieved at lower temperatures, useful coatings on aerospace materials are available.⁵ Silicon nitride was selected for the base material of the bearing elements because of its high melting point, availability as precision bearings, and ongoing efforts to qualify silicon nitride hybrid (metal and ceramic) and all-ceramic bearings for aerospace applications. In addition, a useful diamond coating cannot presently be achieved on common aerospace bearing materials, such as 52100 steel. The results of a bench scale evaluation of diamond-coated silicon nitride bearings operating without additional lubrication is noted in the following.

Experiment

Completed and assembled R8 silicon nitride bearings were obtained consisting of Norton NBD-200 inner and outer rings and Cerbec balls also made of NBD-200. The bearing outer diameter is 3.1 cm with 4-mm-diam balls. Components were prepared for diamond deposition by disassembling the bearing, abrading with 0.1- μm diamond powder, and rinsing in solvents. The diamond scratching procedure is commonly used in CVD diamond deposition processes for enhancing the nucleation density. Diamond growth was achieved in a microwave plasma system operating at 2.45 GHz with a 1% concentration of methane in hydrogen. The total flow rate was 200 standard $\text{cm}^3 \text{ min}^{-1}$ with a pressure of 6.7×10^3 Pa. The sample temperature was measured by a two-color optical pyrometer as approximately 800°C .

Coated components (rings and balls) were examined by optical and scanning electron microscopy (SEM) to determine the coating coverage and microstructure. Raman spectroscopy was performed to determine the diamond quality, providing a nondestructive (optical) evaluation of the coating quality because diamond has a characteristic peak at 1332 cm^{-1} . The film stress can also be determined by Raman spectroscopy as described elsewhere.⁶ Finally, profile

Received Feb. 1, 1997; revision received May 1, 1997; accepted for publication June 1, 1997. Copyright © 1997 by the American Institute of Aeronautics and Astronautics, Inc. All rights reserved.

*Senior Scientist, 3506 Bassett Street. Member AIAA.

measurements were made on the coated balls with a roundness measuring machine.

One bearing set was reassembled and tested without lubrication under nominal load and speed with five balls and a phenolic retainer (Table 1). Excessive torque noise was immediately evident and of sufficient magnitude that the test was terminated after 10 min. The bearing components were disassembled and characterized by optical microscopy, SEM, and Raman spectroscopy to determine the source of premature failure.

Results

SEM characterization of the diamond-coated silicon nitride components prior to bearing assembly indicated a fine-grained microstructure on the balls, inner and outer rings, consistent with their specular appearance. The average diamond grain size of the ball coating was 0.4 μm. The roundness deviation of the coated ball, i.e., sphericity, was measured as 0.13 μm, consistent with a precision bearing ball. However, SEM examination of the tested bearing indicated that film delamination was prevalent on the ball and rings (Fig. 1). Considerable debris was generated by wear of the phenolic retainer. The extent of film failure prompted reevaluation of the feasibility of diamond coating silicon nitride by examining the residual diamond film stress.

The thermal expansion coefficients α of diamond⁷ and silicon nitride are plotted with temperature in Fig. 2, where a surprisingly large temperature dependence is noted for diamond. Generic values of α for silicon nitride were used because the values are expected to vary little among Si₃N₄ materials in comparison to the difference with diamond. The thermal stress in the diamond film σ_{th} arising from cooling to room temperature from the deposition temperature T_{dep} is given by

$$\sigma_{th} = -\frac{E}{1-\nu} \int_{T_{dep}}^{T_m} (\alpha_{diam} - \alpha_{Si_3N_4}) dT \tag{1}$$

where E (= 1050 GPa) and ν (= 0.07) are the Young's modulus and Poisson's ratio of diamond.¹ An intrinsic or growth component may contribute to the total film stress; however, the thermal stress

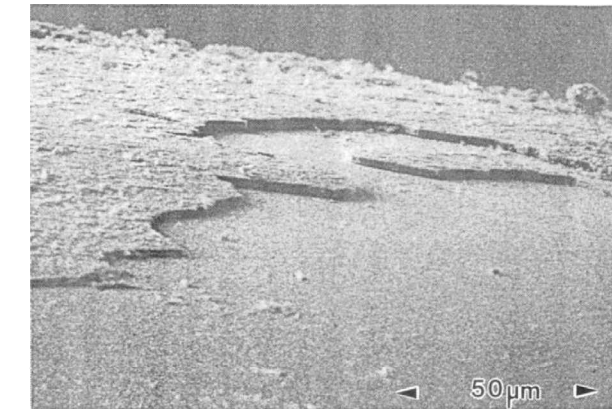


Fig. 1 Scanning electron micrograph of diamond-coated silicon nitride ball after bearing test.

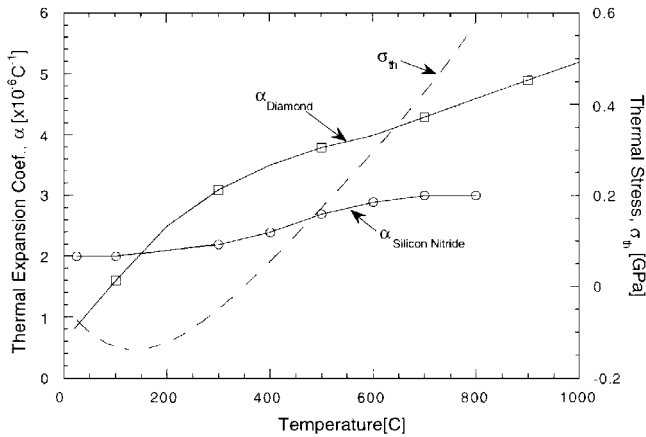


Fig. 2 Thermal expansion coefficient of diamond and silicon nitride with predicted diamond film stress.

predicted by Eq. (1) is found to dominate in other diamond-coated materials.⁶ The dependence of film stress with temperature T follows from the thermal expansion data and is readily given by fitting a polynomial over the range 25°C ≤ T ≤ 800°C (Fig. 2):

$$\begin{aligned} \sigma_{th} = & -3.627 \times 10^{-2} - 1.642 \times 10^{-3} T \\ & + 7.883 \times 10^{-6} T^2 - 9.938 \times 10^{-9} T^3 \\ & + 4.902 \times 10^{-12} T^4 - 1.089 \times 10^{-16} T^5 \text{ GPa} \end{aligned} \tag{2}$$

A tensile film stress is predicted for T_{dep} > 350°C. A tensile film stress was confirmed on coated balls and flat coupons by Raman spectroscopy. The presence of residual tensile film stress precludes the use of diamond-coated silicon nitride for bearing applications because the propensity for film cracking and delamination is enhanced under contact loading. Diamond deposition at reduced temperatures for a compressive film stress on silicon nitride is unavailable with the present technology. Work is ongoing to explore diamond-coated bearing materials, e.g., steel, under compressive film stress.

Acknowledgments

Silicon nitride bearings, test data, and important discussions with P. C. Ward of MPB Corp. are gratefully acknowledged. Thermal expansion data for silicon nitride was supplied by Enceratec Corp. Discussions with J. W. Ager III of the Lawrence Berkeley National Laboratory are also acknowledged.

References

¹Field, J. E., "Appendix: Tables of Properties," *The Properties of Natural and Synthetic Diamond*, edited by J. E. Field, Academic, London, 1992, pp. 667-699.

²Fleischauer, P. D., and Hilton, M. R., "Assessment of the Tribological Requirements of Spacecraft Mechanisms," *Materials Research Society Proceedings*, Vol. 140, Materials Research Society, Pittsburgh, PA, 1989, pp. 9-20.

³Angus, J. C., and Hayman, C. C., "Low-Pressure, Metastable Growth of Diamond and 'Diamond-Like' Phases," *Science*, Vol. 241, Aug. 1988, pp. 913-921.

⁴Drory, M. D., McClelland, R. J., and Ryder, A., "Microstructural Effects on the Performance of CVD Diamond Coatings for Bearing Applications," *2nd International Conference on the Applications of Diamond Films and Related Materials*, MYU, Tokyo, 1993, pp. 207-213.

⁵Drory, M. D., and Hutchinson, J. W., "Diamond Coating of Titanium Alloys," *Science*, Vol. 263, March 1994, pp. 1753-1755.

⁶Ager, J. W., III, and Drory, M. D., "Quantitative Measurement of Residual Biaxial Stress by Raman Spectroscopy in Diamond Grown on a Ti Alloy by Chemical Vapor Deposition," *Physical Review B*, Vol. 48, No. 8, 1993, pp. 2601-2607.

⁷Pickrell, D. J., Kline, K. A., and Taylor, R. E., "Thermal Expansion of Polycrystalline Diamond Produced by Chemical Vapor Deposition," *Journal of Applied Physics*, Vol. 64, No. 18, 1994, pp. 2353-2355.